Feature Extraction and Classification for Remote Sensing Imagery Based on Orthogonal Frequency Division Method

IOP Conf. Series: Materials Science and Engineering **490** (2019) 072022 doi:10.1088/1757-899X/490/7/072022

Feature Extraction and Classification for Remote Sensing Imagery Based on Orthogonal Frequency Division Method

Chenguang Zhang[1,2,a] and Guifa Teng[1,*]

[1]College of Information Science and Technology, Hebei Agricultural University, Baoding, Hebei, China
[2]Department of Computer Science, Haibin College, Beijing Jiaotong University, Cangzhou, Hebei, China

*Corresponding author e-mail: tguifa@126.com
[a]cgzhang@bjtuhbxy.cn

Abstract. Remote sensing (RS) is the unique way to monitor whole world dynamically. Feature extraction and classification for RS image is an important research direction in this field. Image classification is based on feature extraction, and is also the premise of image processing. However, at present, image classification lacks theoretical basis and is still in the stage of visual observation and empirical interpretation. There are many reasons for poor image classification, e.g. lack of clarity or lack of classification basis. In this article, a new method for RS image feature extraction and classification called the "orthogonal frequency division" (OFD) method is proposed. The method combines filtering and stratification, and the experiments prove that it can effectively classify and extract the features of RS images. The traditional filtering methods regard image contents as a whole signal space, after each filtering, only the high frequency values can be separated in the form of edges, while the low frequency values still remains in the signal space, forming an image which pixel values are doubled. If we want to label a region, we have to superimpose these edges, so we need to do filtering for many times, which is a tedious process. Moreover, the scaling ratio is usually small and fixed, therefore, if the differences among regions are large, multiple filtering must be carried out, otherwise the filtering effect is not obvious. Then, although the image compression effect is achieved, the image will become too small and lose its ability to be recognized. The OFD method only needs to be filtered once, its filter group can classify both low and high frequency values and can increase the differences among regions, so that the image contents form layers, different classification results can be extracted by different thresholds. These classification results can be used as the material of neural network training set, at this point, the classification result regions can be labeled directly. By comparing the classification results with some prevailing image processing methods (such as PCA method or wavelet transform method), the classification effect is superior to the traditional methods in terms of classification accuracy.

1. Introduction

Remote sensing [1, 2] technology can detect distant target objects with sensors on RS platforms under the circumstance of contacting with the objects indirectly, especially in harsh or dangerous environments where frequent monitoring is difficult by the common aerial photography [3, 4] technology which logistics costs [5] are high. The narrow sense of RS refers to the detection of the targets' reflected wave or radiation wave, but generalized RS also includes the use of media such as force field, mechanical wave and gravitational field. It can be divided into several categories according to the way of obtaining information [6] and has been widely used in many important fields such as policy making, military affairs and environment detection on the basis of its advantages. With the development of space technology [7], the study of ground observation has been developed from a single, non-related basic subject research into a comprehensive study of multi-level, multi-disciplinary and multi-parameter.

In nowadays, RS is an important research orientation and its applications continue to expand. The property of RS technology is based on two factors: firstly, it depends on the development level of RS platforms and sensors [8]; secondly, it depends on the development level of RS image processing technology. However, current processing level of RS image is far behind sensor collection speed. With the improvement of RS image resolution, image data amount has increased significantly [9], but the corresponding processing technology can hardly adapt to the real-time requirement. In many cases, image processing is still rest on the visual inspection and experience interpretation stage.

Rapid and high-precision image classification [10] is the premise of realizing various practical applications. For this process to be successful, several factors should be considered, e.g. image quality, data amount, a precise classification approach and experts' expertise. Image classification includes two main approaches: supervised [11] and unsupervised [12]. The essential to classification is feature extraction [13]. Generally speaking, image features to be extracted should include many good properties, e.g. good ability to classification, the scale invariance of translation and rotation and so on. With the rapid development of multi-sensor [14] technology, the information contained in RS images is more and more abundant, how to extract topographical information from images and how to make the information useful is an urgent and complex question with regard to RS technology at present.

The image which resolution less than 1 meter is called the hyperspectral image [15, 16, 17], it contains hundreds of different wavelengths in a same area. Its classifier may cause dimensional problem compared with conventional classifiers [18] and the classifier parameters can't be estimated reliably. There are several critical problems in the classification of hyperspectral data: curse of dimensionality, limited number of labeled training samples and large spatial variability of spectral signature [19, 20]. The pixel dimensionality is too high and the classifier requires large training data set, however the numbers of labeled pixels [21, 22] are limited due to complexity and cost of sample collection process.

2. Materials and Methods

Table 1. The OFD Method Design Process

Step 1	Image Data Normalization
Step 1.1	Transform the image into grayscale and set the image size as a square, such as 256*256 pixels.
Step 1.2	Set the image data type to double, and set the data range between 0 and 1.
Step 1.3	Make the image data conform to Gaussian distribution.

$$I(i,j) = \left(I(i,j) - \mu_x\right) \Big/ \sigma_x \tag{2.1}$$

Where:

$$\mu_x = \frac{1}{N \times N} \sum_{i=0}^{N-1} \sum_{j=0}^{N-1} I(i,j) \tag{2.2}$$

$$\sigma_x^2 = \frac{1}{N \times N - 1} \sum_{i=0}^{N-1} \sum_{j=0}^{N-1} \left(I(i,j) - \mu_x \right)^2 \tag{2.3}$$

After normalization, image data conform to Gaussian distribution with mean value of 0 and variance of 1. The correlation function

$$C_X(I_i, I_j) = R_X(I_i, I_j) - \mu_x(I_i)\mu_x(I_j) \tag{2.4}$$

Step 2	Set Sliding Window
Step 2.1	Set the size of sliding window to 2*2 pixels.
Step 2.2	Let the value of sliding window as equation (2.5)

$$A = \begin{pmatrix} a_1^T \\ a_2^T \end{pmatrix} = \begin{bmatrix} a & b \\ c & d \end{bmatrix} \tag{2.5}$$

At this point, the eigenvalues and eigenvectors of sliding window can be represented as

$$d = \begin{bmatrix} \lambda_1 & 0 \\ 0 & \lambda_2 \end{bmatrix}, V = (v_1, v_2) = \begin{bmatrix} v_{11} & v_{12} \\ v_{21} & v_{22} \end{bmatrix} \tag{2.6}$$

The following conclusions can be obtained from the properties of eigenvalues and eigenvectors:

$$Av_i = V \begin{bmatrix} \lambda_1 & 0 \\ 0 & \lambda_2 \end{bmatrix} = (\lambda_1 v_1, \lambda_2 v_2), i = 1, 2 \tag{2.7}$$

$$VV^T = V^T V = E \tag{2.8}$$

$$v_{11}^2 + v_{21}^2 = v_{12}^2 + v_{22}^2 = 1 \tag{2.9}$$

$$v_{11} \times v_{12} = -v_{21} \times v_{22} \tag{2.10}$$

$$v_{11} \times v_{21} = -v_{12} \times v_{22} \tag{2.11}$$

The equation (2.7) is equivalent of the projection from A to V, and V is basis. If A is treated as an input signal, then A contains two time series:

$$a_1 = \{X_1(t_1), X_1(t_2)\} = (a, b) \tag{2.12}$$

$$a_2 = \{X_2(t_1), X_2(t_2)\} = (c, d) \tag{2.13}$$

The equation (2.12) equivalent to a signal which abscissa is “a” and which ordinate is “b”, and the projection from A to v1 is $\lambda_1 v_1$. In the same way, the equation (2.13) equivalent to a signal which abscissa is “c” and which ordinate is “d”, and the projection from A to v2 is $\lambda_2 v_2$. Matrix V can also be expressed as a two-dimensional coordinate system. According to equation (2.7), the abscissa of v_1 is v_{11}, the ordinate of v_1 is v_{21}, and the length of v_1 is 1. Similarly, the abscissa of v_2 is v_{12}, the ordinate of v_2 is v_{22}, and the length of v_2 is 1. So the length of V is $\sqrt{2}$, V is always on a circle which radius is $\sqrt{2}$. After projection, the norm can be represented as:

$$H(Z) = |H(Z)| \cdot Z^{J(\theta)} \tag{2.14}$$

Where:

$$|H(Z)| = \sqrt{\lambda_1^2 v_1^2 + \lambda_2^2 v_2^2} \tag{2.15}$$

$$\theta = \arctan \frac{|v_{21}|}{|v_{11}|} - \arctan \frac{\left| \lambda_2 \cdot \sqrt{v_{12}^2 + v_{22}^2} \right|}{\left| \lambda_1 \cdot \sqrt{v_{11}^2 + v_{21}^2} \right|} \tag{2.16}$$

If V is used to filter rows and columns of A, it could be represented as

$$V^T AV = \begin{bmatrix} v_{11} & v_{21} \\ v_{12} & v_{22} \end{bmatrix} \begin{bmatrix} a & b \\ c & d \end{bmatrix} \begin{bmatrix} v_{11} & v_{12} \\ v_{21} & v_{22} \end{bmatrix} = \begin{bmatrix} av_{11}^2 + bv_{11}v_{21} + cv_{11}v_{21} + dv_{21}^2 & av_{11}v_{12} + bv_{11}v_{22} + cv_{12}v_{21} + dv_{21}v_{22} \\ av_{11}v_{12} + bv_{12}v_{21} + cv_{11}v_{22} + dv_{21}v_{22} & av_{12}^2 + bv_{12}v_{22} + cv_{12}v_{22} + dv_{22}^2 \end{bmatrix} \tag{2.17}$$

According to equation (2.8), in coordinate system, v_{11} and v_{12} are perpendicular to v_{21} and v_{22} respectively. Combined with equation (2.10) and (2.11), above result can be simplified as

$$= \begin{bmatrix} av_{11}^2 + dv_{21}^2 & (a-d)v_{11}v_{12} \\ (a-d)v_{11}v_{12} & av_{12}^2 + dv_{22}^2 \end{bmatrix} \Leftrightarrow \begin{bmatrix} av_{11}^2 + dv_{21}^2 & (d-a)v_{21}v_{22} \\ (d-a)v_{21}v_{22} & av_{12}^2 + dv_{22}^2 \end{bmatrix} \tag{2.18}$$

It can be seen that after filtering, the values of main diagonal equivalent to the projection of signal "a" and "d" on basis elements. At this point, the effect of signal "b" and "c" is removed, this process equivalent to a two-valued downsampling, or it equivalent to a time series which effect is related only to the initial and final status but not to the intermediate status. The values of secondary diagonal are expressed by the subtraction between "a" and "d", and the sign of product result of basis elements. If A is a symmetric matrix, the values on secondary diagonal are 0. The effect of secondary diagonal equivalent to taking the partial derivatives of the values after downsampling and then projecting them on the basis, which can be expressed as equation (2.19).

$$\frac{\partial^2 f}{\partial x \partial y} v_{21} v_{22}, or, -\frac{\partial^2 f}{\partial x \partial y} v_{11} v_{12} \tag{2.19}$$

This formula can describe the process of image edge detection. Since the basis element "V_{ij}" is signed number, the final result can be positive only if the product of two horizontal elements is different from the second partial derivative of the function, or the product of two vertical elements and the second partial derivative of the function are the same, then the extracted edge can be normally displayed.

Step 3	Set Filter Group as equation (2.20)

$$\omega_{i,j} = \frac{v_{i,j}}{|v_{i,j}|} \cdot \frac{v_j}{\sqrt{\sum_{i=1}^{2} \sum_{j=1}^{2} v_{i,j}^2}}, i = 1,2; j = 1,2 \tag{2.20}$$

Where: ω is the low-pass filter if $v_{1,j} * v_{2,j} > 0$, its function is to calculate the mean of local data, so as to make local data more smooth. Otherwise, ω is the high-pass filter if $v_{1,j} * v_{2,j} < 0$, its function is to get partial derivatives of local data, this process is usually replaced by the subtraction.

For each sliding window, the high frequency and low frequency values are random. The generation of the filter group is corresponding to current window, but not fixed. The high-pass and low-pass filtering results will appear randomly on either of two positions of main diagonal. Therefore, two images will be formed after filtering, and the two images are complementary. That is to say, for the same position on main diagonal, if it is high-pass filtering result in first image, it must be low-pass filtering result in second image, and vice versa. Therefore, if the two images are superimposed, the original image will be restored.

After filtering, the two values on the main diagonal are high-pass filtering result (dark) or low-pass filtering result (bright), while the two values on the secondary diagonal are edge detection results. Moreover, the processed image size will be reduced to half of the original, thus achieving image compression effect.

In practice, $\lambda_1 >> \lambda_2$ or $\lambda_1 << \lambda_2$, according to equation (2.6) and equation (2.18), the high-pass and low-pass filtering results can be replaced directly by $\max(\lambda_1, \lambda_2)$ and $\min(\lambda_1, \lambda_2)$, and the norm of projection is:

$$\sqrt{\lambda_1^2 v_1^2 + \lambda_2^2 v_2^2} \approx \max(\lambda_1 v_1, \lambda_2 v_2) = \max(\lambda_1, \lambda_2) \tag{2.21}$$

becauseλ_1 and λ_2 usually differ much, the larger party takes the lead. The complementary effect of high-pass and low-pass filtering results are show as equation (2.22).

$$A_1 = v_1^T A v_1 \qquad A_2 = v_2^T A v_2 \qquad A = A_1 + A_2 \tag{2.22}$$

Where:

$$v_1 = \begin{bmatrix} -|v_{11}| & +|v_{12}| \\ -|v_{21}| & -|v_{22}| \end{bmatrix}, or, v_1 = \begin{bmatrix} +|v_{11}| & -|v_{12}| \\ +|v_{21}| & +|v_{22}| \end{bmatrix}$$

$$v_2 = \begin{bmatrix} +|v_{11}| & +|v_{12}| \\ -|v_{21}| & +|v_{22}| \end{bmatrix}, or, v_2 = \begin{bmatrix} -|v_{11}| & -|v_{12}| \\ +|v_{21}| & -|v_{22}| \end{bmatrix} \tag{2.23}$$

The values on the main diagonal of A_1 are the low-pass filtering results and high-pass filtering results respectively. The values on the main diagonal of A_2 are high-pass filtering results and low-pass filtering results respectively. A is the original image restored after two images are superimposed.

The complementary effect of the filter in equation (2.20) could be combined to form the new filter in equation (2.24). After filtering, the first position in sliding window is the low-pass filtering result, and the other three positions are the high-pass filtering results. The first position should be retained, while the others should be removed, which is more conducive to the subsequent classification work. At this point, the size of original image is reduced to half.

$$\omega_{i,j} = \delta_{i,j} \cdot \eta_{i,j} \cdot \left| v_{i,j} \right| \tag{2.24}$$

Where:

$$\delta_{i,j} = \begin{cases} 1, \dfrac{v_{1,j}}{v_{2,j}} > 0 \\ -1, \dfrac{v_{1,j}}{v_{2,j}} < 0 \end{cases}, \eta_{i,j} = \begin{cases} -1, \dfrac{v_{i,j}}{\left| v_{i,j} \right|} = 1 \\ 1, \dfrac{v_{i,j}}{\left| v_{i,j} \right|} = -1 \end{cases}$$

Step 4	Increase Filtering Effect

In order to make the differences among filter results more obvious, the filter should be further adjusted. Exponential function has obvious effect on high frequency value, while logarithmic function has obvious effect on low frequency value. Since the low-pass filtering result is retained in equation (2.24), the logarithmic function should be selected for processing.

$$\omega(i,j) = \log_2^{\left(\left(\omega(i,j) - \mu_x \right)^2 / \sigma_x^2 \right)} \tag{2.25}$$

So far, the filtered image has shown obvious stratification characteristics. The filtering results in the same region are less different, while the filtering results in different regions are more different. Moreover, the maximum is allowed to be greater than 1 and the minimum is allowed to be less than 0 (in original image, 1 is the maximum and 0 is the minimum). For example, assuming that the pond and the road are next to each other, both of them are highlighted and appear as a whole, but it is possible that the pond's filtering result is 2 and the road's filtering result is 70 (both of them are greater than 1). At this point, it is difficult to classify and extract each region by a single filtering method. The traditional filtering method has some limitations. Taking wavelet transform as an example, firstly, the image scaling coefficient is fixed, if a feature value is between the original image and the coefficient, the feature is likely to be directly crossed and cannot be found and extracted in filtering process. Secondly, after each filtering, the size of image will be reduced to half, while the pixel value will be doubled. This change is for the image as a whole , not for local. In other words, if two regions in the image are very similar, they will also be very similar after filtering. Therefore, the difficulty of classification is not reduced. Thirdly, if the filtering results of a region are very small, it must be filtered several times before it can be separated from the black background color, which is a tedious process. Therefore, the hierarchical processing method is better than the single filtering method, which can classify all image regions at one time and simplify the multiple filtering processes.

$$sub = \max\left(\max\left(image\right)\right) - \min\left(\min(image\right) \tag{2.26}$$

Where: the variable "image" represents the image to be processed at this time.

$$temp = round(sqrt(sub)) \tag{2.27}$$

Where: the variable "temp" represents the layers level of the image to be divided. If:

$$\begin{aligned} \text{image}(i, j) \in [&\text{minimum(image)+sub/temp*level1}, \\ &\text{minimum(image)+sub/temp*level2}) \end{aligned} \tag{2.28}$$

Then mark the image regions which meet the requirement. Where: level1 and level2 are the upper and lower limits of image classification interval. The output marked image is the desired. The image after being classified can be used as training sample of neural network, which can directly be labeled, and the meaning of each region needs to be marked by experts.

3. Results

In order to meet the needs of follow-up work, this paper chose the hyperspectral remote sensing image of Fuping county (Baoding city, Hebei province, China) as the experimental data. The resolution of image is 0.26 meters.

Figure 1. Separate Buildings from Trees

The classification effect of Figure 1 is obtained by classifier (2.28). According to the calculation, the original image is divided into 22 grades (this value is not fixed, the greater the difference among regions in original image, the greater the classification levels. However, in general, this classification method is too detailed, so that each classification level can only represent a part of target region. Therefore, it is necessary to combine appropriate levels to form the overall effect of a target region). The black background in second image represents trees, which are the combined effect of grade 0 through 5. The black background in third image represents buildings, which are the combined effect of grade 5 through 12. The fourth image is a useless region separated from original image. Many traditional methods cannot separate this region from buildings, while the OFD method can separate effectively, which indicates that the OFD method has more accurate classification ability.

Figure 2. Separate Buildings from Fields

The second image and the third image are difficult to be separated by traditional methods, because the two regions are very similar. Through observation, it can be found that although both regions are fields, the region represented by the second image is darker than that of the third one because there are many plants. Moreover, the traditional methods cannot separate the buildings from surrounding land, but the OFD method can separate the buildings to achieve the classification effect of the fourth image.

Figure 3. Filtering Effect of Roads and Plants

The first image is the original image. The second image shows dark colored trees. The third image shows lighter colored grass. The fourth image shows the transition section on both sides of road. The fifth image shows road.

4. Discussion

4.1 Advantages of OFD Method

The filtering operation only needs to be done once, avoiding the definition of the basis function, which is often difficult to define in practice.

The form of the filter is not fixed, but varies dynamically according to the content of each sliding window. The filter can separate the high frequency from the low frequency so that the low frequency can be directly separated from the signal space. The high frequency exists in the form of edge, while the low frequency exists in the form of region, which is more conducive to classification operations.

Image classification is conducted in a hierarchical manner. Different from the traditional filtering method, the traditional filtering method USES multi-resolution analysis, adopts the high-frequency filter when the time domain is reduced, and USES the low-frequency filter when the time domain is enlarged, so as to adjust the precision of the filtering. The OFD method stratifies the filtering results each time, and merges the similar levels of attributes, and finally gets the classification results.

4.2 Comparison of Classification Results

In this section, some prevailing image processing methods (such as PCA method and wavelet transform method) are compared with OFD method to verify the classification effect of each method.

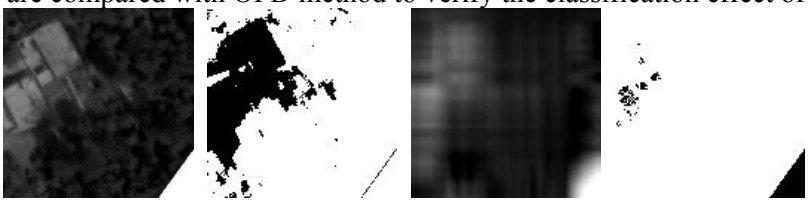

Figure 4. Contrast Effect

The first image is the original image. The second image shows the effect of OFD method. The third image shows the effect of PCA method. The fourth image shows the effect of wavelet transform.

Figure 4 shows the effect of separating buildings from trees. The difficulty of this process lies in: first, from the remote sensing image, trees and buildings are very similar and difficult to distinguish; second, parts of the building are obscured by trees and do not show regular edges.

According to the classification results, the OFD method can separate the building regions along the irregular edges. Most of the buildings appear brighter, but areas close to the trees are relatively dark, probably because of the trees' shadows. The OFD method is not affected by the shadow, which extracts all the buildings.

The classification effect of PCA method is relatively fuzzy, and the result selects the first three main components of the order. One drawback of the PCA method is how to select principal components. If the number of principal components is kept too much, the computational amount will increase and cannot achieve the effect of simplification. However, if the number of principal components is kept too little, information will be lost too much.

The classification result of wavelet transform only extracts a small part of the building, and the triangular area without content in the lower right corner of the image is also included in the classification result, resulting in wrong data.

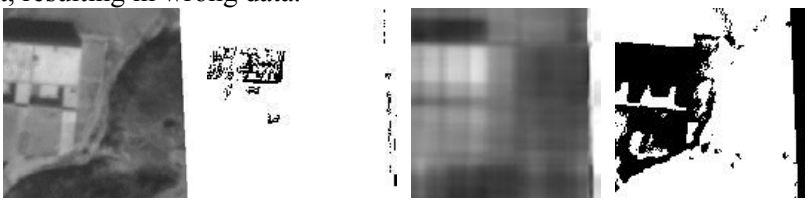

Figure 5. Contrast Effect II

The display order of the processing results is the same as that in Figure 4. It can be seen from the results that the wavelet transform method cannot distinguish the building from the surrounding land, while the OFD method can extract the building more precisely.

In Figure 6, it can be seen from the processing results that the OFD method and the wavelet transform method have similar effects on the extraction of buildings, but in the upper left and lower right corner of the image, the land in the original image is also extracted as a building by the wavelet transform method, while the OFD method does not extract redundant land areas.

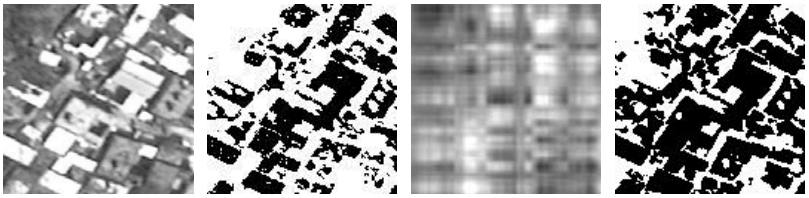

Figure 6. Contrast Effect III

According to Figure 7, the wavelet transform cannot separate the road from the surrounding grassland, while the OFD method can accurately separate the road.

Figure 7. Contrast Effect IV

5. Conclusions

In this paper, a remote sensing image feature extraction and classification method called orthogonal frequency division method is proposed. The sliding window can be filtered by the corresponding filter group according to its content. Different from the traditional filtering method, the filter designed in this paper can directly extract the low-frequency signal and form a region, thus providing convenience for subsequent classification work. The filtering process only needs to be carried out once to avoid the redundancy of traditional filtering methods. Filtering results are orthogonal, eliminating the interaction among various factors. The difference between each part of filtering results is increased, and combined with the hierarchical processing method, the parts with similar attributes are merged into one class, and finally the image classification effect is achieved. In this paper, the classification effect of OFD method is compared with that of PCA method and wavelet transform method, and the experimental results show that OFD method has more accurate classification effect.

Acknowledgments

I would like to thank my mentor, Guifa Teng. For his excellent academic attainments and rigorous academic attitude, have helped me lot.

References

[1] Blaschke, T. 2010. Object based image analysis for remote sensing. ISPRS JOURNAL OF PHOTOGRAMMETRY AND REMOTE SENSING 65(1): 2-16.
[2] Melgani, F; Bruzzone, L. 2004. Classification of hyperspectral remote sensing images with support vector machines. IEEE TRANSACTIONS ON GEOSCIENCE AND REMOTE SENSING 42(8): 1778-1790.
[3] Sandmann, H; Lertzman, KP. 2003. Combining high-resolution aerial photography with gradient-directed transects to guide field sampling and forest mapping in mountainous terrain. FOREST SCIENCE 49(3): 429-443.
[4] Ask, P; Nilsson, SG. 2004. Stand characteristics in color-infrared aerial photographs as indicators of epiphytic lichens. BIODIVERSITY AND CONSERVATION 13(3): 529-542.
[5] Colomina, I.; Molina, P. 2014. Unmanned aerial systems for photogrammetry and remote sensing: A review. ISPRS Journal of Photogrammetry and Remote Sensing 92(2): 79-97.

[6] Arts, Koen; van der Wal, Rene; Adams, William M. 2015. Digital technology and the conservation of nature. Ambio 44(suppl 4): 661-673.
[7] Winker, DM; Couch, RH; McCormick, MP. 1996. An overview of LITE: NASA's lidar in-space technology experiment. PROCEEDINGS OF THE IEEE 84(2): 164-180.
[8] Jimenez-Munoz, Juan C.; Sobrino, Jose A.; Skokovic, Drazen et al. 2014. Land Surface Temperature Retrieval Methods from Landsat-8 Thermal Infrared Sensor Data. IEEE GEOSCIENCE AND RS LETTERS 11(10): 1840-1843.
[9] Pope, Allen; Rees, W. Gareth; Fox, Adrian J. et al. 2014. Open Access Data in Polar and Cryospheric Remote Sensing. Remote Sensing 6(7): 6183-6220.
[10] Russakovsky, Olga; Deng, Jia; Su, Hao et al. 2015. ImageNet Large Scale Visual Recognition Challenge. INTERNATIONAL JOURNAL OF COMPUTER VISION 115(3): 211-252.
[11] Cheriyadat, Anil M. 2013. Unsupervised Feature Learning for Aerial Scene Classification. IEEE Transactions on Geoscience & RS 52(1): 439-451.
[12] Han, Junwei; Zhang, Dingwen; Cheng, Gong et al. 2015. Object Detection in Optical Remote Sensing Images Based on Weakly Supervised Learning and High-Level Feature Learning. IEEE TRANSACTIONS ON GEOSCIENCE AND REMOTE SENSING 53(6): 3325-3337.
[13] Burke, Michael; Lasenby, Joan. 2015. Pantomimic Gestures for Human-Robot Interaction. IEEE Transactions on Robotics 31(5): 1225-1237.
[14] Guay, Kevin C.; Beck, Pieter S. A.; Berner, Logan T. et al. 2014. Vegetation productivity patterns at high northern latitudes: a multi-sensor satellite data assessment. GLOBAL CHANGE BIOLOGY 20(10): 3147-3158.
[15] Bioucas-Dias, Jose M.; Plaza, Antonio; Camps-Valls, Gustavo et al. 2013. Hyperspectral Remote Sensing Data Analysis and Future Challenges. IEEE GEOSCIENCE AND REMOTE SENSING MAGAZINE 1(2): 6-36.
[16] Bioucas-Dias, Jose M.; Plaza, Antonio; Dobigeon, Nicolas et al. 2012. Hyperspectral Unmixing Overview: Geometrical, Statistical, and Sparse Regression-Based Approaches. IEEE JOURNAL OF SELECTED TOPICS IN APPLIED EARTH OBSERVATIONS AND RS 5(2): 354-379.
[17] Plaza, Antonio; Benediktsson, Jon Atli; Boardman, Joseph W. et al. 2009. Recent advances in techniques for hyperspectral image processing. RS OF ENVIRONMENT 113(1): S110-S122.
[18] Serpico, Sebastiano B.; Moser, Gabriele. 2007. Extraction of Spectral Channels from Hyperspectral Images for Classification Purposes. IEEE Transactions on Geoscience and RS 45(2): 484-495.
[19] Chen, Yushi; Lin, Zhouhan; Zhao, Xing et al. 2014. Deep Learning-Based Classification of Hyperspectral Data. IEEE JOURNAL OF SELECTED TOPICS IN APPLIED EARTH OBSERVATIONS AND RS 7(6): 2094-2107.
[20] Camps-Valls, G; Bruzzone, L. 2005. Kernel-based methods for hyperspectral image classification. IEEE Trans. Geosci. Remote Sens. 43(6): 1351–1362.
[21] Yao, Xiwen; Han, Junwei; Cheng, Gong et al. 2016. Semantic Annotation of High-Resolution Satellite Images via Weakly Supervised Learning. IEEE TRANSACTIONS ON GEOSCIENCE AND RS 54(6): 3660-3671.
[22] Guillaumin, Matthieu; Kuettel, Daniel; Ferrari, Vittorio. 2014. ImageNet Auto-Annotation with Segmentation Propagation. INTERNATIONAL JOURNAL OF COMPUTER VISION 110(3): 328-348.